
Article:
Ros, F.C., Reeves-McLaren, N. orcid.org/0000-0002-1061-1230, Masó, N. et al. (1 more author) (2019) Synthesis, structure and dielectric properties of a new family of phases, ABC3O11 : A = La, Pr, Nd, Sm, Gd; B = Zr, Hf; C = Ta, Nb. Journal of the Australian Ceramic Society, 55 (2). pp. 305-314. ISSN 2510-1560

https://doi.org/10.1007/s41779-018-0236-x

- *Authors*

Fadhlina Che Ros, Nik Reeves-McLaren, Nahum Masó and Anthony R West

- *Title*

Synthesis, structure and dielectric properties of a new family of phases, ABC_3O_{11}: A = La, Pr, Nd, Sm, Gd; B = Zr, Hf; C = Ta, Nb

- *Affiliations and addresses of authors*

Nik Reeves-McLaren, Anthony R West

Department of Materials Science and Engineering, Mappin Street, University of Sheffield, Sheffield S13JD, United Kingdom

Nahum Masó

Institute of Chemical Technology (ITQ), Technical University of Valencia (UPV), Camino de Vera, s/n 46022, Valencia, Spain

Corresponding author

Fadhlina Che Ros

Physics Department, Centre for Defence Foundation Studies, National Defence University of Malaysia, Sungai Besi Camp, 57000 Kuala Lumpur, Malaysia

fadhlina@upnm.edu.my

Tel: +603-90514437

Abstract:

Eight new phases with the general formula of ABC_3O_{11} with different rare-earth, (Zr, Hf), (Nb, Ta) combinations, have been prepared by solid-state reactions at a temperature range of 1200^o – 1500^o C. The new phases: LaHfTa, LaHfNb, LaZrNb, PrHfTa, NdHfTa, NdHfNb, SmHfTa and GdHfTa are characterised by X-ray and neutron diffraction data at room temperature and variable frequency impedance measurements. They are isostructural with $LaZrTa_3O_{11}$ which consist of alternating single layers of UO_7 pentagonal bipyramids and octahedra as shown by Rietveld refinement of X-ray and neutron powder diffraction data. Lattice parameters decrease with decreasing size of rare earth elements substitution at A-site and of all, Gd is the smallest rare earth that formed $LaZrTa_3O_{11}$ analogues. Detailed attempts of attained and unattainable $LaZrTa_3O_{11}$ analogues with different temperatures are included in this paper. All phases are highly insulating with temperature-independent bulk permittivities in the range 17 to 50; LaHfNb demonstrates the highest permittivity. Arrhenius plot shows that the activation energies are in the range 0.8 to 1.94 eV.

Keywords: U_3O_7 pentagonal bipyramids; Rare-earth; Low permittivity; Rietveld refinement

- *Acknowledgments*

We thank EPSRC and The Ministry of Higher Education of Malaysia for their financial support through the research grant of Fundamental Research Grant Scheme (FRGS) no. FRGS/1/2017/STG07/UPNM/02/2.

Introduction

The crystal structure of $LaZrTa_3O_{11}$ was first reported [1] in 1991 and was indexed on an orthorhombic unit cell, a = 10.890(3) Å, b = 12.450(3) Å and c = 6.282(2) Å. However, its true symmetry was subsequently shown to be hexagonal with a geometrically-related unit cell and space group $P6_322$ (N° 182) with a = 6.2824(2) Å, c = 12.4469 Å and Z = 2 [2].

$LaZrTa_3O_{11}$ is isostructural with $CaTa_4O_{11}$ [3] which belongs to a series of compounds [4] with general formula $Me_x(Nb,Ta)_{3n+1}O_{8n+3}$, e.g. n = 1: $CaTa_4O_{11}$, $Na_2Nb_4O_{11}$, $Na_2Ta_4O_{11}$, $K_2Ta_4O_{11}$, $Ag_2Nb_4O_{11}$, $Ag_2Ta_4O_{11}$ and "$Cu_2Ta_4O_{11}$"; n = 2: $RETa_7O_{19}$ where RE = La – Eu, Y and Bi; intergrowth of 1 and 2: $Cu_5Ta_{11}O_{30}$. These phases are structurally-related to α-U_3O_8 whose structure exhibits layers of UO_7 pentagonal bipyramids sharing edges in the equatorial plane and apical oxygens [5]. These layers are repeated identically in the perpendicular direction. However, the $LaZrTa_3O_{11}$ structure has an alternating single layer of (Ta, Zr)O_7 pentagonal bipyramids with layers containing (Ta, Zr)O_6 octahedra and LaO_8 polyhedron; consecutive (Ta, Zr)O_7 layers are rotated by 180° relative to each other. La occupies an octahedral *2c* site and a 3:1 disordered distribution of Ta and Zr occupy *6g* pentagonal bipyramidal and *2d* octahedral sites. Figure 1 illustrates the layers of pentagonal bypiramids alternating with octahedra. $LaZrTa_3O_{11}$ is highly insulating with electrical conductivity as low as 3×10^{-7} ohm^{-1} cm^{-1} at 800 °C[1].

Given the ferroelectric and antiferroelectric nature of some structurally-related materials [6–9], namely $Ag_2Nb_4O_{11}$, $Na_2Nb_4O_{11}$ and its solid solution $(Na_{1-x}Ag_x)Nb_4O_{11}$, it has been of interest to seek other members of this structural family and to evaluate their electrical properties. In this work, the synthesis of phases isostructural with $LaZrTa_3O_{11}$ with the general formula of ABC_3O_{11}; A = La^{3+}, Pr^{3+}, Nd^{3+}, Sm^{3+}, Gd^{3+}, B = Zr^{4+}, Hf^{4+} and C = Ta^{5+}, Nb^{5+} is reported. Structure determination by Rietveld refinement of several of the new phases were determined using X-ray and neutron powder diffraction data. A preliminary measurement of their electrical properties was made using impedance spectroscopy.

Experimental

Starting materials were Ta_2O_5, Nb_2O_5, ZrO_2, HfO_2, La_2O_3, Pr_6O_{11}, Nd_2O_3 (99.9% pure, Stanford Materials) and Sm_2O_3, Gd_2O_3 (99.9% pure, Sigma Aldrich). They were dried at 800° – 1000° C and stored under vacuum. Mixtures totalling 3 – 5 g were weighed, mixed with acetone using an agate mortar and pestle, dried, pressed into pellets and fired in Pt crucibles in the air in electric muffle furnaces. The mixtures were heated at different times and temperatures in the range 1000° – 1500° C for up to 3 days; intermittently. Pellets were removed from the furnace, crushed into a fine powder, repelleted and returned to the furnace. Reaction conditions were determined by trial and error, taking account of the refractory nature of the oxide reagents which meant that long period at high temperatures were required for the reaction to occur. Not any of the compositions, Table 1 are single phase products. The residual amounts of secondary phases remained, even after repeated firing. However, a relatively small amount of impurity is negligible for some compositions since they barely affect the results.

Phase analysis by X-ray powder diffraction (XRD) was carried out using a STOE Stadi P diffractometer, $CuK\alpha_1$ radiation (λ = 1.54056 Å). NIST 640d Si was used as an external standard for line position calibration. Data were processed and compared against reference data in the ICDD's PDF-2 database using the WinX^{POW} software package. Room temperature time-of-flight (ToF) neutron powder diffraction (ND) data were collected on the General Materials diffractometer, (GEM) at the ISIS facility, Rutherford Appleton Laboratory, RAL, Oxford for $LaHfNb_3O_{11}$ powder in a vanadium can. Data were collected in the backscattering detector bank (50.07° - 74.71°), bank 4 with resolution $\Delta Q/Q \sim 0.79 \times 10^{-2}$. Rietveld refinement was performed using the EXPGUI interface for GSAS and both XRD and ND data.

For electrical measurements, cylindrical sintered pellets were coated with Pt paste electrodes on opposite faces and hardened by heating in the air at 800° C for 2 h. The samples, with electrodes attached, were placed in a ceramic compression jig inside a furnace controlled and measured to ± 1° C. Impedance spectroscopy (IS) measurements were performed using Hewlett Packard 4192A and Solartron 1260/1286 impedance analysers at frequencies 10 Hz - 1 MHz and 1 kHz - 1 MHz,

respectively. Impedance data were recorded between room temperature and 800° C in the air with 100 mV applied *ac* voltage. Data were corrected for overall pellet geometry and for the blank cell capacitance (jig correction) and analysed using the software program ZView.

Results and Discussion

Reaction Conditions and Products

Results of the attempted synthesis of new phases with different rare-earth – Zr, Hf – Nb, Ta combinations are summarised in Table 1. Eight new phases, in addition to $LaZrTa_3O_{11}$, were prepared and for each, the synthesis conditions are detailed. Attempted synthesis of a further 12 new phases was unsuccessful; details of the reaction conditions and products, in which there was no evidence of formation of a phase with the $LaZrTa_3O_{11}$ structure, are given in Table 1(b).

The new phases were readily recognised by the similarity of their XRD patterns to that of $LaZrTa_3O_{11}$. Powder XRD patterns of these new phases are shown in Figures 2 and 3 for the Ta-based and Nb-based compositions, respectively. Indexed data for one analogue, $LaHfTa_3O_{11}$, are given in Table 2; data for all the analogue have been submitted for inclusion in the ICDD powder diffraction file. Unit cell data are summarised in Table 3.

The lattice parameters decreased on the substitution of La by smaller rare earth elements. Gd was the smallest rare earth that formed $LaZrTa_3O_{11}$ analogue. With three cationic components in each phase: rare earth, Zr/Hf and Nb/Ta, there is a complex interplay between ion size, possible formation of $LaZrTa_3O_{11}$ analogue and its thermal stability. It was found that a standard set of synthesis conditions could not be used for all the new phases. In general, higher reaction temperatures (~ 1500° C) were required to obtain Ta-based phases compared to the reaction temperatures needed for the Nb analogues (1200° – 1300° C), consistent with the lower reactivity of Ta_2O_5 compared to Nb_2O_5. However, fewer Nb-based family members were prepared successfully, and those that did form had less thermal stability than the Ta analogues and decomposed at above ~ 1400° C.

For Ta-based phases, $LaHfTa_3O_{11}$ was the easiest to prepare and obtain as a phase with $LaZrTa_3O_{11}$ structure, whereas the smaller rare earths require increasingly longer reaction times and lower temperatures. $SmHfTa_3O_{11}$ and $GdHfTa_3O_{11}$ started to form at 1200° C, as shown by the traces of $LaZrTa_3O_{11}$ patterns in the XRD data. The impurity phases remained similar until 1400° C, although peak intensities decreased with time, Sm, Gd target phases were still not phase-pure and decomposed after increasing the temperature to 1500° C.

In the niobate systems, only three compositions produced $LaZrTa_3O_{11}$ analogues: $LaHfNb_3O_{11}$, $LaZrNb_3O_{11}$ and $NdHfNb_3O_{11}$, which are all formed at temperatures in the range 1150° – 1300° C. These niobates have lower thermal stability than their corresponding tantalates. $LaHfNb_3O_{11}$ has an upper limit of stability at 1300° C before melting at 1350° C, $NdHfNb_3O_{11}$ appears to have an upper limit of stability at ~ 1200° C and $LaZrNb_3O_{11}$ appears to be on the edge of stability at 1150° C. The presence of $LaZrTa_3O_{11}$ phase was detected after ~ 36 h but decomposed to $LaNb_3O_9$ after another 12 h of reaction time.

Structure Refinements

Rietveld refinement using XRD data was carried out for three compositions: $LaHfTa_3O_{11}$, $PrHfTa_3O_{11}$ and $NdHfTa_3O_{11}$. For the fourth composition, $LaHfNb_3O_{11}$, combined refinement using XRD and ND data was conducted. For each refinement, the crystal structure of $LaZrTa_3O_{11}$ was used as the starting model with La on octahedral *2c* sites, Ta and Hf disordered in a fixed 1:3 ratio on octahedral *6g* and *2d* sites and oxygen on *4f*, *6g* and *12i* sites. Total occupancies for all sites were fixed at unity; background and peak profile parameters were refined first using the Chebyschev function with ten terms for the background. This was followed by the single positional variable for the *6g* site and simultaneous refinement of the isotropic thermal parameters, U_{iso}, of the cation sites until convergence, with negligible shifts in atomic variables.

The statistical measures and visual fits shown in Figures 4 – 7 were relatively good. For $LaHfTa_3O_{11}$, $\chi^2 = 4.704$, R factors < 7% and thermal, or U_{iso}, parameters were all refined to acceptable, positive

values. For $PrHfTa_3O_{11}$ and $NdHfTa_3O_{11}$, good fits were also obtained with acceptable statistical measures. U_{iso} values were positive for all atoms, indicating that the statistical occupancies of Ta, Hf over both sites is reasonable; with the χ^2 value for $PrHfTa_3O_{11}$ at 7.475 compared to 5.996 for $NdHfTa_3O_{11}$. The final atomic coordinates and bond distances are presented in Tables 4 and 5. The un-reacted HfO_2 peak in $LaHfTa_3O_{11}$ and $PrHfTa_3O_{11}$ was so small that it could barely affect the refinements with the weight fraction 0.165% and 0.047%, respectively. As for $NdHfTa_3O_{11}$, impurities of $NdTa_3O_9$ and un-reacted HfO_2 are taken into account with weight fraction 1.236% and 0.774%, respectively; with the lattice parameters obtained for $NdTa_3O_9$: a = 3.9127(9) Å, c = 7.865(3) Å.

For $LaHfNb_3O_{11}$, the ToF ND data were collected at room temperature. The background, diffractometer constant DIFA, and peak profiles were refined for the ToF histogram with fixed values of lattice parameters and unit cell volume, which were then refined together with atomic positions and U_{iso}, with initial values of 0.005 $Å^2$. The whole process was repeated until convergence. Combined structure refinement gave a good visual fit and statistical measures (Figure 7, Table 4), although χ^2 was inconsiderably high, 5.878.

These new phases are isostructural with $LaZrTa_3O_{11}$ which contains two layers of pentagonal bipyramids related by the 6_3 symmetry axis sharing edges. Both octahedral layers, i.e. (Ta/Nb, Hf/Zr)(1)O_7 and (Ta/Nb, Hf/Zr)(2)O_6 contain a disordered 3:1 ratio of Ta/Nb and Hf/Zr, where (Ta/Nb, Hf/Zr)(1)O_7 at z = 0 and ½ corner-share four of their oxygens, O(1) and O(2) with each other and have two apical oxygens, O(3) along the z-axis. Meanwhile, (Ta/Nb, Hf/Zr)-O_6 and REO_6 octahedra that are located at z = ¼ and ¾ are formed by the apical oxygens; three in the layer below and above (Ta/Nb, Hf/Zr)(1)-O_7 octahedra.

Electrical Properties

Impedance measurements for several of the new phases over the range from room temperature to 800° C showed that are all excellent insulators. The permittivities of ABC_3O_{11} are in the range $17 \leq \varepsilon' \leq 50$ and are essentially frequency – independent over the range 10^4 to 10^7 Hz, Figure 8. The highest

permittivity is shown by $LaHfNb_3O_{11}$, ~ 50, whilst the lowest is $SmHfTa_3O_{11}$, ~ 17. The capacitance data of the tantalates from room temperature to 400 ºC were independent of frequency and temperature. The conductivity of all the samples was too low to measure at room temperature with the available instrumentation, indicative of highly insulating materials with R >> 10^9 Ωcm. At higher temperatures, the conductivity data were obtained from IS measurements and are shown as Arrhenius plots in Figure 9. The highest conductivity was found for $LaHfNb_3O_{11}$, ~ 10^{-5} $\Omega^{-1}cm^{-1}$ at 1000 K. The activation energy, E_a for conduction obtained from the gradient of the Arrhenius plots was in the range 0.8 and 1.94 eV.

Figure 10 shows the bulk permittivity, ε_∞, of the tantalates phases at room temperature plotted against ionic radii of rare earth elements. The bulk permittivity decreased with decreasing ionic radius; replacing Ta^{5+} by Nb^{5+} in one case increased the permittivity significantly.

Conclusions

A new family of phases based on $LaZrTa_3O_{11}$ with the general formula of ABC_3O_{11}: A = La, Pr, Nd, Sm; B = Zr, Hf and C = Ta, Nb, but not all combinations, has been prepared by solid state reaction. The successful elements combinations are LaHfTa, LaHfNb, LaZrNb, PrHfTa, NdHfTa, NdHfNb, NdZrNb, SmHfTa and GdHfTa. However, none were completely in phase pure as ATa_3O_9 and un-reacted raw materials were often present. Similar to $LaZrTa_3O_{11}$, all new phases were indexed on the hexagonal space group $P6_322$; unit cell parameters and cell volume decreased with decreasing size of A.

The temperatures necessary for the sample synthesis depend on the size of A and C. Most AHfTa combinations were prepared at 1500º C except for SmHfTa and GdHfTa which were prepared at 1400º C and decomposed at 1500º C. $AHfNb_3O_{11}$ compounds were prepared at 1150º – 1300º C, which was significantly lower than required to synthesise the tantalates. With smaller rare earth ions, it was generally found to be increasingly difficult to eliminate secondary phases. Gd appears to be the smallest rare earth that allows formation of $LaZrTa_3O_{11}$ analogue phases.

The crystal structures have been confirmed by Rietveld refinement using both XRD and NPD data in space group $P6_322$. All four structures that were refined contain a random distribution of (Ta, Nb) and Hf in the ration 3:1 over the two sites of edge-sharing octahedra.

All samples were insulating at room temperature and higher temperatures were required to obtain conductivity data. The activation energies are in the range 0.8 – 1.74 eV, consistent with the insulating nature of the materials. The capacitances of all the samples, in the form of sintered pellets, are frequency – independent at low temperatures, and gradually increased as the temperature increased. Of all the samples, $LaHfNb_3O_{11}$ exhibits the highest permittivity ~ 50. There was no evidence of any ferroic transitions, but it would be interesting to measure the low temperature electrical properties of $LaHfNb_3O_{11}$.

Acknowledgments

We thank EPSRC and The Ministry of Higher Education of Malaysia for financial support through the research grant of Fundamental Research Grant Scheme (FRGS) no. FRGS/1/2017/STG07/UPNM/02/2.

References

1. Zheng, C. and West, A.R.: Compound and solid solution formation, phase equilibria and electrical properties in the ceramic system $ZrO_2 – La_2O_3 – Ta_2O_5$. J. Mater. Chem. 1, 163-167 (1991)

2. Grins, J., Nygren, M., Zheng, C. et al.: Structure of $LaZrTa_3O_{11}$, a $CaTa_4O_{11}$ isotype. Mat. Res. Bull. 27, 141-145 (1992)

3. Jahnberg, L.: Crystal structures of $Na_2Nb_4O_{11}$ and $CaTa_4O_{11}$. J. Solid State Chemistry. 1, 454-462 (1970)

4. Jahnberg, L.: A series of structures based on stacking of α-U_3O_8-type layers of MO_7 pentagonal bipyramids. Mat. Res. Bull. 16, 513-518 (1981)

5. Loopstra, B.O.: Neutron diffraction investigation of U_3O_8. Acta Cryst. 1964;17: 651-654.

6. Masó, N. and West, A.R.: A new family of ferroelectric materials: $Me_2Nb_4O_{11}$ (Me = Na and Ag) J. Mater. Chem. 20, 2082-2084 (2010)

7. Masó, N., Woodward, D.I., Thomas, P.A. et al.: Structural characterisation of ferroelectric $Ag_2Nb_4O_{11}$ and dielectric $Ag_2Ta_4O_{11}$. J. Mater. Chem. 21, 2715-2722 (2011)

8. Masó, N., Woodward, D.I., Thomas, P.A., et al.: Polymorphism, structural characterisation and electrical properties of $Na_2Nb_4O_{11}$. J. Mater Chem. 21, 12096-12102 (2011)

9. Masó, N. and West, AR.: Dielectric properties, polymorphism, structural characterisation and phase diagram of $Na_2Nb_4O_{11}$–$Ag_2Nb_4O_{11}$ solid solutions. J. Solid State Chem. 225, 438-449 (2015)

X-ray powder diffraction data for $LaHfTa_3O_{11}$ (LHT)

2θ(obs)	*h k l*	*2θ(calc)*	*Obs - calc*	*Int.*	*d (obs) Å*	*d (calc) Å*
14.240	0 0 2	14.229	0.0108	31.0	6.2149	6.2196
16.280	1 0 0	16.287	-0.0066	49.0	5.4402	5.4380
17.797	1 0 1	17.787	0.0106	6.6	4.9798	4.9827
21.709	1 0 2	21.691	0.0187	19.8	4.0904	4.0939
27.050	1 0 3	27.020	0.0296	4.0	3.2937	3.2973
28.728	0 0 4	28.683	0.0454	57.0	3.1050	3.1098
29.328	1 1 1	29.315	0.0131	89.6	3.0428	3.0442
31.910	1 1 2	31.904	0.0054	100.0	2.8023	2.8028
33.170	1 0 4	33.159	0.0119	12.2	2.6986	2.6996
35.868	1 1 3	35.847	0.0217	31.8	2.5016	2.5030
39.613	2 0 3	39.605	0.0076	2.1	2.2733	2.2737
40.819	1 1 4	40.808	0.0103	2.9	2.2089	2.2094
43.638	0 0 6	43.622	0.0157	4.8	2.0725	2.0732
44.029	2 1 0	44.021	0.0085	6.2	2.0550	2.0554
44.647	2 1 1	44.649	-0.0018	8.4	2.0280	2.0279
46.549	1 1 5	46.538	0.0113	27.5	1.9494	1.9499
46.879	1 0 6	46.861	0.0185	3.1	1.9365	1.9372
49.459	2 1 3	49.453	0.0055	4.2	1.8413	1.8415
50.299	3 0 0	50.295	0.0034	32.8	1.8126	1.8127
52.549	3 0 2	52.544	0.0051	4.9	1.7401	1.7403
52.880	1 1 6	52.878	0.0015	31.0	1.7300	1.7301
53.389	2 1 4	53.389	-0.0000	6.3	1.7147	1.7147
55.728	2 0 6	55.710	0.0181	6.5	1.6481	1.6436
58.174	2 1 5	58.173	0.0016	4.0	1.5845	1.5846
58.938	3 0 4	58.928	0.0104	35.6	1.5658	1.5651
59.299	2 2 1	59.285	0.0140	11.6	1.5571	1.5575
59.749	1 1 7	59.747	0.0016	13.4	1.5455	1.5455
60.799	2 2 2	60.806	-0.0076	14.1	1.5223	1.5221
61.400	3 1 0	61.425	-0.0245	5.1	1.5038	1.5032
61.964	3 1 1	61.924	0.0399	4.1	1.4954	1.4973
63.289	2 2 3	63.294	-0.0046	7.9	1.4632	1.4631
63.709	2 1 6	63.705	0.0043	3.1	1.4595	1.4596
65.869	3 1 3	65.840	0.0294	2.1	1.4168	1.4174
68.749	3 0 6	68.732	0.0174	2.7	1.3643	1.3646
69.168	3 1 4	69.170	-0.0013	5.0	1.3571	1.3571
69.928	2 1 7	69.922	0.0060	2.8	1.3442	1.3443
70.932	4 0 2	70.898	0.0332	6.0	1.3276	1.3281
73.344	3 1 5	73.347	-0.0023	2.2	1.2898	1.2897
75.020	1 1 9	75.025	-0.0054	4.9	1.2651	1.2650
75.979	2 2 6	75.975	0.0039	8.8	1.2515	1.2515
76.369	4 0 4	76.396	-0.0269	2.6	1.2450	1.2457
76.790	2 1 8	76.806	-0.0153	2.8	1.2403	1.2400
78.050	3 2 2	78.062	-0.0120	4.4	1.2234	1.2232
78.889	1 0 10	78.876	0.0132	1.8	1.2124	1.2126

Crystal symmetry: hexagonal
Refined cell: a = 6.28319(6) Å, α = 90.0°, (a = b)
c = 12.4358(2) Å, γ = 120.0°,
V = 425.173(8) Å^3

X-ray powder diffraction data for $PrHfTa_3O_{11}$ (PHT)

2θ (obs)	*h k l*	*2θ (calc)*	*Obs - calc*	*Int.*	*d (obs) Å*	*d (calc) Å*
14.276	0 0 2	14.265	0.0106	30.1	6.1992	6.2038
16.337	1 0 0	16.331	0.0067	50.4	5.4213	5.4235
17.835	1 0 1	17.834	0.0005	7.1	4.9694	4.9695
21.760	1 0 2	21.748	0.0114	20.8	4.0811	4.0832
27.090	1 0 3	27.092	-0.0018	4.6	3.2890	3.2887
28.775	0 0 4	28.757	0.0172	55.6	3.1001	3.1019
29.402	1 1 1	29.395	0.0075	86.3	3.0353	3.0361
31.997	1 1 2	31.991	0.0059	100.0	2.7949	2.7954
33.259	1 0 4	33.246	0.0124	13.3	2.6917	2.6926
35.953	1 1 3	35.994	0.0089	32.2	2.4959	2.4965
39.722	2 0 3	39.714	0.0088	2.5	2.2673	2.2678
40.927	1 1 4	40.919	0.0073	3.8	2.2033	2.2037
43.746	0 0 6	43.739	0.0072	5.4	2.0676	2.0679
44.152	2 1 0	44.144	0.0075	6.8	2.0496	2.0499
44.332	2 0 4	44.333	-0.0013	4.4	2.0417	2.0416
44.774	2 1 1	44.775	-0.0010	9.8	2.0225	2.0225
46.665	2 1 2	46.626	0.0383	28.3	1.9449	1.9464
46.997	1 0 6	46.988	0.0094	3.5	1.9319	1.9323
49.598	2 1 3	49.593	0.0053	4.7	1.8365	1.8367
50.438	3 0 0	50.439	-0.0005	35.1	1.8079	1.8078
52.697	3 0 2	52.694	0.0030	5.1	1.7356	1.7357
53.029	1 1 6	53.025	0.0034	33.8	1.7255	1.7256
53.541	2 1 4	53.541	0.0009	6.9	1.7102	1.7102
55.868	2 0 6	55.867	0.0011	7.2	1.6443	1.6444
58.341	2 1 5	58.340	0.0012	4.5	1.5804	1.5804
59.097	3 0 4	59.098	-0.0015	37.4	1.5620	1.5619
59.488	2 2 1	59.459	0.0288	13.3	1.5526	1.5533
59.921	1 1 7	59.917	0.0042	14.7	1.5424	1.5425
60.983	2 2 2	60.985	-0.0028	15.7	1.5181	1.5180
61.604	3 1 0	61.607	-0.0031	5.8	1.5043	1.5042
62.145	3 1 1	62.108	0.0376	5.1	1.4925	1.4933
63.482	2 2 3	63.481	0.0005	8.4	1.4642	1.4642
63.884	2 1 6	63.891	-0.0064	3.9	1.4560	1.4558
66.037	3 1 3	66.037	-0.0004	2.5	1.4136	1.4136
66.886	2 2 4	66.888	-0.0022	2.1	1.3977	1.3977
68.938	3 0 6	68.937	0.0012	3.2	1.3610	1.3611
69.368	3 1 4	69.379	-0.0113	6.0	1.3537	1.3535
70.122	2 1 7	70.131	-0.0085	3.8	1.3409	1.3408
71.140	4 0 2	71.116	0.0236	7.2	1.3242	1.3246
73.572	3 1 5	73.572	-0.0002	3.0	1.2863	1.2863
75.251	1 1 9	75.251	-0.0002	5.8	1.2618	1.2618
76.209	2 2 6	76.210	-0.0012	10.1	1.2483	1.2482
76.635	4 0 4	76.635	0.0002	3.6	1.2424	1.2424
[illegible]	[illegible]	[illegible]	-0.0152	3.4	1.2370	1.2368
[illegible]	[illegible]	[illegible]	0064	5.1	1.2200	1.2200

Crystal symmetry: hexagonal
Refined cell: a = 6.281145(8) Å, α = 90.0°, (a = b)
c = 12.4412(2) Å, γ = 120.0°,
V = 425.08(3) Å^3

X-ray powder diffraction data for $NdHfTa_3O_{11}$ (NHT)

2θ(obs)	*h k l*	*2θ(calc)*	*Obs - calc*	*Int.*	*d (obs) Å*	*d (calc) Å*
14.285	0 0 2	14.279	0.0063	29.2	6.1952	6.1979
16.344	1 0 0	16.346	-0.0019	48.1	5.4191	5.4185
17.852	1 0 1	17.851	0.0012	6.9	4.9645	4.9649
21.768	1 0 2	21.769	-0.0009	20.2	4.0795	4.0793
27.109	1 0 3	27.118	-0.0085	4.5	3.2866	3.2856
28.790	0 0 4	28.785	0.0047	53.7	3.0985	3.0990
29.418	1 1 1	29.423	-0.0049	84.9	3.0337	3.0332
32.019	1 1 2	32.022	-0.0032	100.0	2.7930	2.7828
33.281	1 0 4	33.279	0.0018	13.7	2.6899	2.6901
35.980	1 1 3	35.979	0.0005	31.6	2.4941	2.4941
39.770	2 0 3	39.753	0.0171	3.2	2.2647	2.2656
40.963	1 1 4	40.960	0.0033	3.9	2.2014	2.2016
43.784	0 0 6	43.783	0.0006	5.8	2.0660	2.0660
44.173	2 1 0	44.188	-0.0144	7.2	2.0486	2.0480
44.359	2 0 4	44.377	-0.0188	4.6	2.0405	2.0397
44.809	2 1 1	44.819	-0.0100	9.8	2.0210	2.0206
46.702	2 1 2	46.673	0.0294	28.5	1.9434	1.9446
47.030	1 0 6	47.035	-0.0058	3.9	1.9306	1.9304
49.638	2 1 3	49.643	-0.0050	4.6	1.8351	1.8350
50.477	3 0 0	50.490	-0.0130	34.1	1.8066	1.8062
52.743	3 0 2	52.748	-0.0045	5.3	1.7342	1.7340
53.079	1 1 6	53.080	-0.0007	33.5	1.7240	1.7240
53.585	2 1 4	53.595	-0.0099	7.4	1.7089	1.7086
55.914	2 0 6	55.924	-0.0104	7.7	1.6431	1.6428
58.395	2 1 5	58.400	-0.0053	4 8	1.5791	1.5789
59.150	3 0 4	59.160	-0.0099	37.6	1.5607	1.5605
59.548	2 2 1	59.520	0.0276	13.5	1.5512	1.5519
59.977	1 1 7	59.980	-0.0027	14.0	1.5411	1.5411
61.038	2 2 2	61.049	-0.0112	16.1	1.5169	1.5166
61.655	3 1 0	61.671	-0.0153	6.2	1.5031	1.5028
62.195	3 1 1	62.172	0.0230	5.4	1.4914	1.4919
63.542	2 2 3	63.548	-0.0055	8.8	1.4630	1.4629
63.954	2 1 6	63.958	-0.0043	4.0	1.4546	1.4545
66.090	3 1 3	66.107	-0.0171	2.8	1.4126	1.4123
69.006	3 0 6	69.011	-0.0057	3.7	1.3599	1.3598
69.434	3 1 4	69.454	-0.0193	6.3	1.3525	1.3522
70.202	2 1 7	70.207	-0.0050	3.9	1.3396	1.3395
71.211	4 0 2	71.193	0.0181	6.6	1.3231	1.3234
73.639	3 1 5	73.653	-0.0134	3.2	1.2853	1.2851
75.337	1 1 9	75.335	0.0015	6.4	1.2605	1.2606
76.287	2 2 6	76.295	-0.0075	10.0	1.2472	1.2471
76.728	4 0 4	76.720	0.0082	3.8	1.2411	1.2412
77.104	2 1 8	77.128	-0.0242	3.5	1.2360	1.2357
78.384	3 2 2	78.397	-0.0136	5.8	1.2190	1.2188
79.203	1 0 10	79.207	-0.0042	2.8	1.2084	1.2084

Crystal symmetry: hexagonal

Refined cell: $a = 6.2578(1)$ Å, $\alpha = 90.0^o$, ($a = b$)

$c = 12.3938(3)$ Å, $\gamma = 120.0^o$,

$V = 420.32(2)$ Å^3

X-ray powder diffraction data for $SmHfTa_3O_{11}$ (SHT)

2θ(obs)	*h k l*	*2θ(calc)*	*Obs - calc*	*Int.*	*d (obs) Å*	*d (calc) Å*
14.305	0 0 2	14.325	-0.0200	28.6	6.1867	6.1782
16.380	1 0 0	16.398	-0.0182	47.9	5.4073	5.4014
17.894	1 0 1	17.908	-0.0142	6.9	4.9531	4.9492
21.841	1 0 2	21.839	0.0021	19.7	4.0660	4.0664
27.188	1 0 3	27.206	-0.0181	6.0	3.2773	3.2752
28.897	0 0 4	28.880	0.0175	52.9	3.0873	3.0891
29.530	1 1 1	29.518	0.0112	82.7	3.0225	3.0237
32.140	1 1 2	32.126	0.0138	100.0	2.7828	2.7839
33.406	1 0 4	33.388	0.0176	14.4	2.6801	2.6815
36.114	1 1 3	36.097	0.0163	32.5	2.4852	2.4862
36.280	2 0 2	36.273	0.0069	15.3	2.4741	2.4746
40.083	1 0 5	40.092	-0.0097	4.1	2.2477	2.2472
41.112	1 1 4	41.096	0.0164	4.7	2.1938	2.1946
43.952	0 0 6	43.930	0.0217	6.5	2.0584	2.0594
44.344	2 1 0	44.335	0.0085	8.1	2.0411	2.0415
44.541	2 0 4	44.526	0.0150	5.4	2.0326	2.0332
44.980	2 1 1	44.969	0.0108	11.1	2.0138	2.0142
46.878	2 1 2	46.829	0.0491	31.1	1.9365	1.9384
47.210	1 0 6	4.195	0.0151	4.7	1.9237	1.9243
49.815	2 1 3	49.811	0.0043	5.9	1.8290	1.8292
50.667	3 0 0	50.661	0.0061	37.7	1.8002	1.8005
52.938	3 0 2	52.928	0.0100	6.4	1.7282	1.7285
53.274	1 1 6	53.262	0.0121	34.2	1 7181	1.7185
53.784	2 1 4	53.779	0.0052	8.9	1.7030	1.7032
56.132	2 0 6	56.118	0.0138	9.1	1.6372	1.6376
58.614	2 1 5	58.604	0.0101	5.9	1.5737	1.5739
59.373	3 0 4	59.366	0.0071	40.0	1.5554	1.5555
59.780	2 2 1	59.728	0.0524	15.7	1.5457	1.5470
60.201	1 1 7	60.191	0.0098	15.7	1.5359	1.5362
61.271	2 2 2	61.263	0.0078	16.7	1.5117	1.5118
61.899	3 1 0	61.887	0.0120	7.6	1.4978	1.4981
62.429	3 1 1	62.391	0.0375	7.0	1.4864	1.4872
63.779	2 2 3	63.773	0.0063	10.5	1.4581	1.4582
64.182	2 1 6	64.186	-0.0041	5.5	1.4499	1.4498
66.336	3 1 3	66.344	-0.0074	4.1	1.4080	1.4078
69.269	3 0 6	69.262	0.0073	4.9	1.3553	1.3555
69.695	3 1 4	69.706	-0.0110	7.5	1.3481	1.3479
70.479	2 1 7	70.464	0.0154	5.3	1.3350	1.3353
71.489	4 0 2	71.453	0.0362	9.2	1.3186	1.3192
73.924	3 1 5	73.925	-0.0012	4.7	1.2811	1.2811
75.648	1 1 9	75.618	0.0297	7.5	1.2561	1.2565
76.595	2 2 6	76.581	0.0136	11.5	1.2429	1.2431
77.018	4 0 4	77.008	0.0096	5.7	1.2372	1.2373
77.427	2 1 8	77.419	0.0073	5.4	1.2316	1.2317
78.709	3 2 2	78.694	0.0150	7.4	1.2148	1.2150

Crystal symmetry: hexagonal
Refined cell: $a = 6.23885(8)$ Å, $\alpha = 90.0^o$, ($a = b$)
$c = 12.3569(2)$ Å, $\gamma = 120.0^o$,
$V = 416.53(1)$ Å^3

X-ray powder diffraction data for $GdHfTa_3O_{11}$ (GHT)

2θ(obs)	*h k l*	*2θ(calc)*	*Obs - calc*	*Int.*	*d (obs) Å*	*d (calc) Å*
14.381	0 0 2	14.343	0.0376	27.8	6.1543	6.1703
16.452	1 0 0	16.417	0.0351	48.8	5.3836	5.3950
17.951	1 0 1	17.930	0.0209	7.3	4.9376	4.9433
21.891	1 0 2	21.866	0.0249	19.3	4.0569	4.0615
27.208	1 0 3	27.240	-0.0322	6.0	3.2750	3.2712
28.924	0 0 4	28.917	0.0074	55.3	3.0844	3.0852
29.568	1 1 1	29.554	0.0138	85.4	3.0187	3.0201
32.177	1 1 2	32.165	0.0113	100.0	2.7797	2.7806
33.437	1 0 4	33.431	0.0062	14.3	2.6777	2.6782
34.043	2 0 1	33.992	0.0512	5.1	2.6314	2.6353
36.153	1 1 3	36.143	0.0104	32.4	2.4825	2.4832
40.225	1 0 5	40.145	0.0805	4.8	2.2401	2.2444
41.155	1 1 4	41.149	0.0062	5.2	2.1916	2.1919
43.981	0 0 6	43.989	-0.0083	7.5	2.0571	2.0568
44.400	2 1 0	44.390	0.0102	8.8	2.0387	2.0391
45.031	2 1 1	45.025	0.0063	12.0	2.0116	2.0118
46.924	2 1 2	46.888	0.0363	33.0	1.9347	1.9361
49.873	2 1 3	49.874	-0.0016	6.8	1.8270	1.8270
50.732	3 0 0	50.724	0.0080	37.2	1.7981	1.7983
52.942	3 0 2	52.995	-0.0534	7.4	1.7281	1.7265
53.335	1 1 6	53.334	0.0015	33.8	1.7163	1.7163
53.849	2 1 4	53.849	0.0004	9.0	1.7011	1.7011
56.191	2 0 6	56.194	-0.0033	9.3	1.6357	1.6356
58.675	2 1 5	58.682	-0.0073	7.7	1.5722	1.5720
59.452	3 0 4	59.444	0.0079	39.5	1.5535	1.5537
59.851	2 2 1	59.805	0.0460	17.5	1.5441	1.5452
60.267	1 1 7	60.274	-0.0066	16.0	1.5344	1.5342
61.354	2 2 2	61.343	0.0107	17.4	1.5098	1.5101
61.976	3 1 0	61.968	0.0083	8.0	1.4961	1.4963
62.507	3 1 1	62.473	0.0349	7.8	1.4847	1.4854
63.860	2 2 3	63.858	0.0028	10.9	1.4565	1.4565
64.286	2 1 6	64.274	0.0119	6.4	1.4478	1.4481
66.451	3 1 3	66.432	0.0183	5.1	1.4058	1.4062
69.359	3 0 6	69.358	0.0010	5.8	1.3538	1.3538
69.781	3 1 4	69.801	-0.0193	7.9	1.3466	1.3463
70.570	2 1 7	70.563	0.0067	5.9	1.3335	1.3336
71.584	4 0 2	71.550	0.0343	9.0	1.3171	1.3176
74.034	3 1 5	74.029	0.0048	5.7	1.2795	1.2795
75.717	1 1 9	75.730	-0.0124	8.4	1.2551	1.2550
76.685	2 2 6	76. 691	-0.0057	11.5	1.2417	1.2416
77.140	4 0 4	77.116	0.0234	6.2	1.2355	1.2358
78.826	3 2 2	78.804	0.0220	7.7	1.2132	1.2135
79.587	1 0 10	79.631	-0.0444	4.8	1.2036	1.2030

Crystal symmetry: hexagonal
Refined cell: $a = 6.2293(1)$ Å, $\alpha = 90.0^o$, ($a = b$)
$c = 12.3421(3)$ Å, $\gamma = 120.0^o$,
$V = 414.77(2)$ Å^3

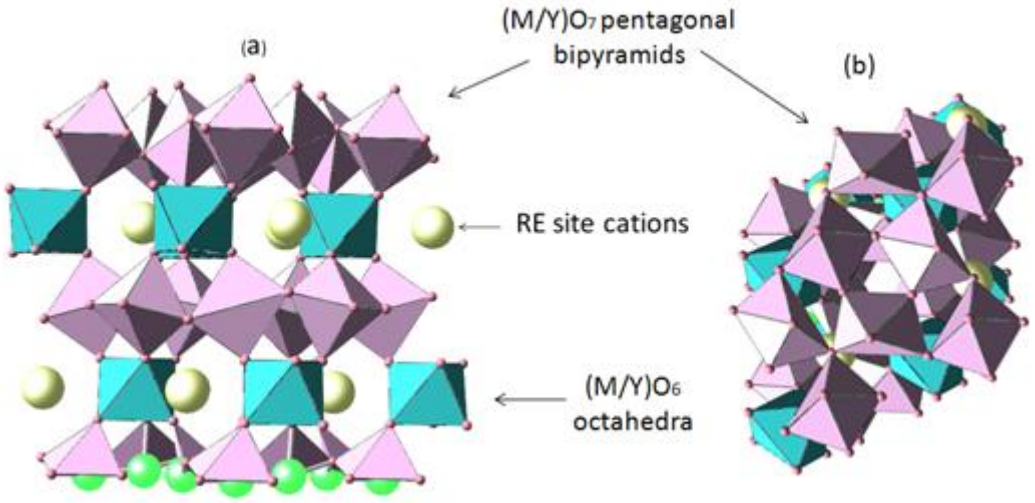

Figure 1: (a) Stacking sequence of single layers of pentagonal bipyramids alternate with single layers of octahedral layers and (b) layer of pentagonal bipyramids at $z = 0$.

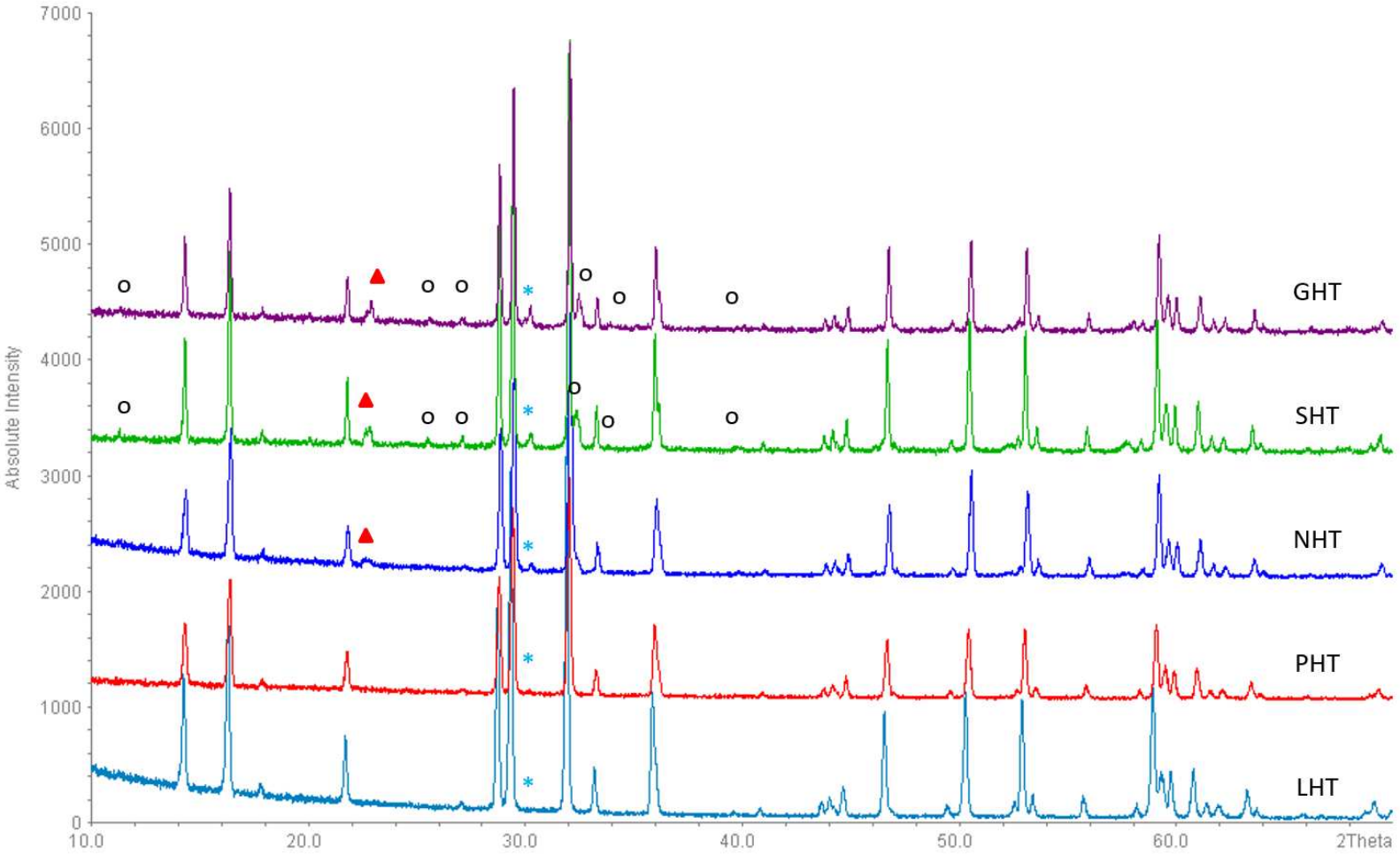

Figure 2: XRD profiles of $AHfTa_3O_{11}$ compositions, (*) indicates un-reacted HfO_2, (▲) indicates un-reacted Ta_2O_5 and (o) indicates ATa_3O_9.

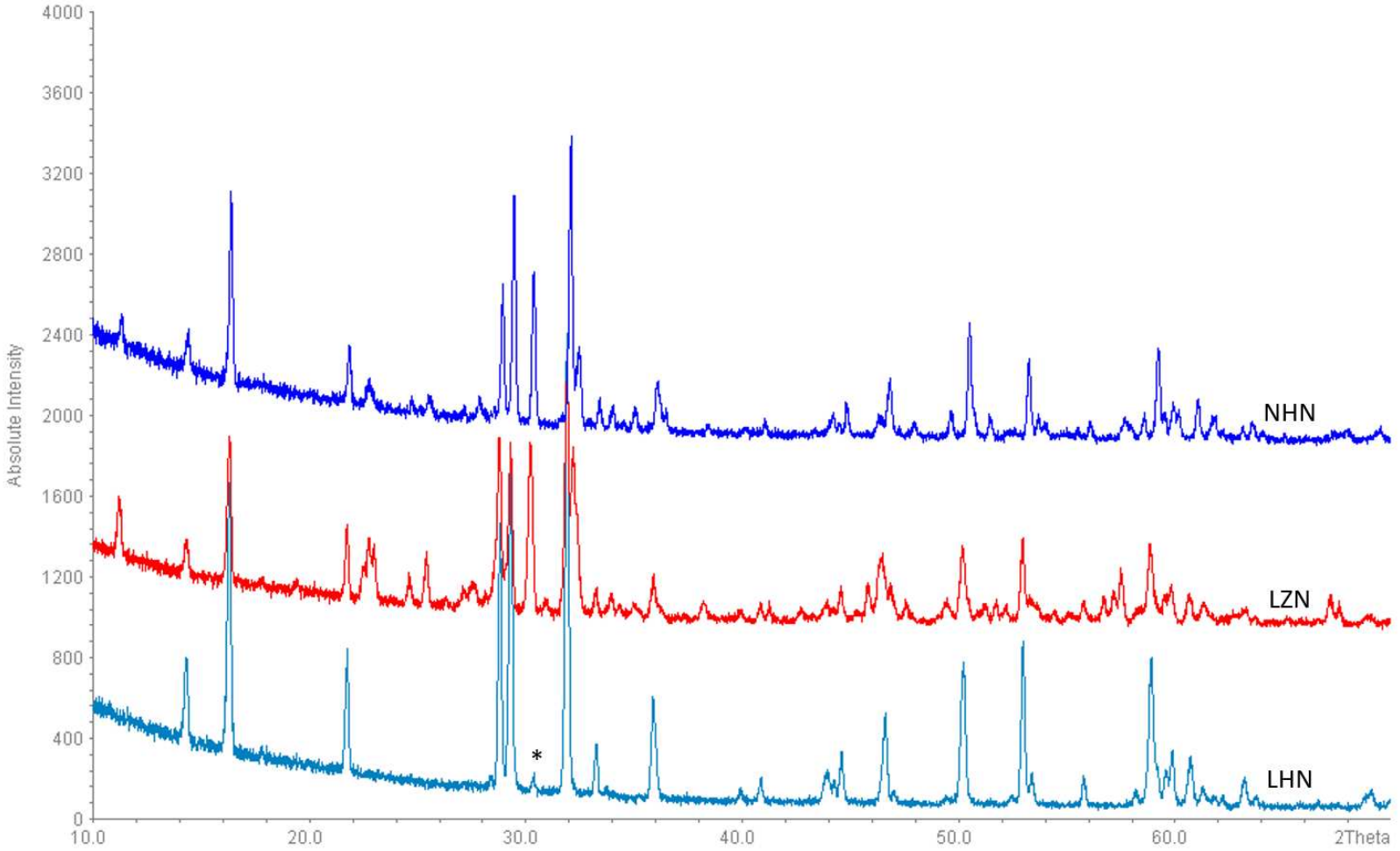

Figure 3: XRD profiles of $ABNb_3O_{11}$ compositions, LHN contains un-reacted HfO_2 (*), whereas LZN and NHN are mixed phases.

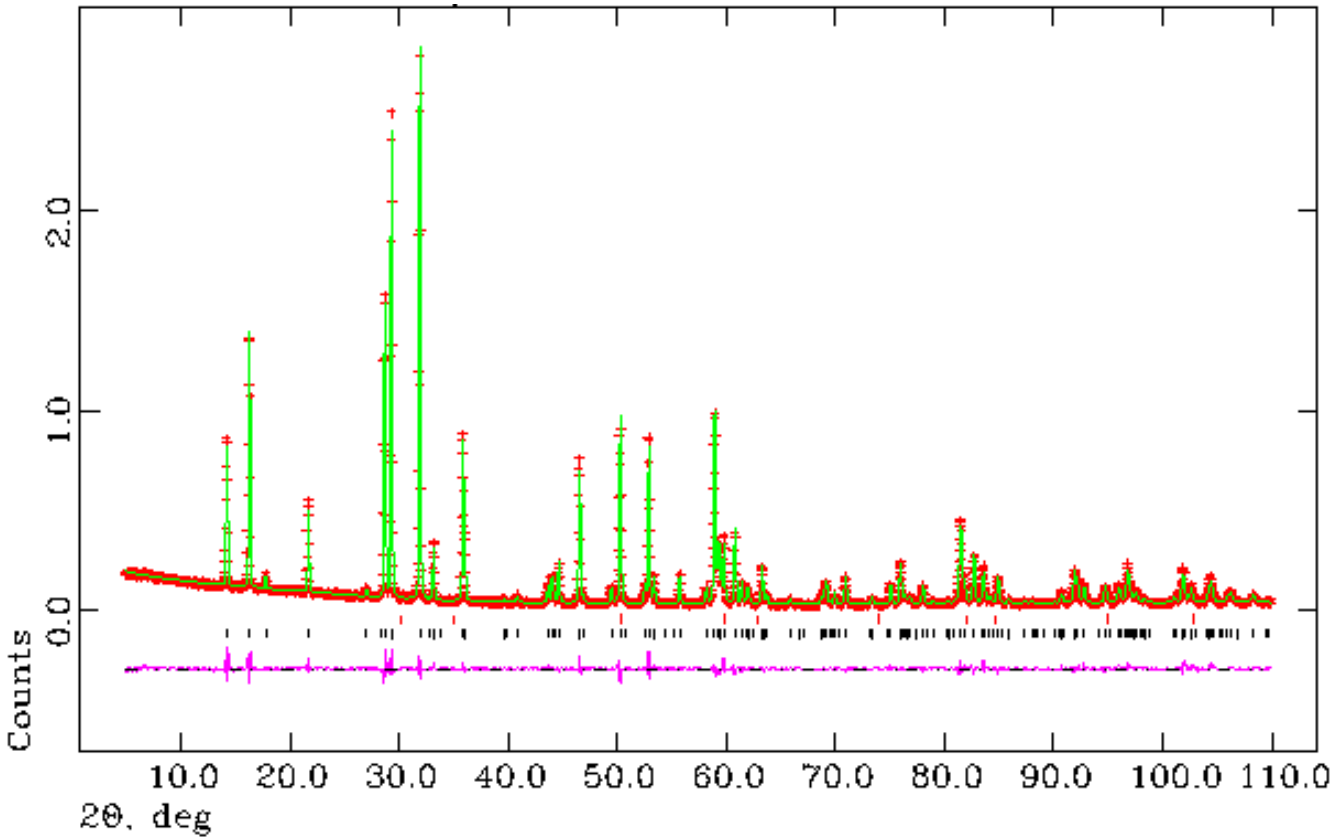

Figure 4: The observed (+), calculated (-) and difference (-) profiles from Rietveld refinement of $LaHfTa_3O_{11}$ with a disordered arrangement of Ta, Hf in the ratio 3:1. Ticks marks represent Bragg peak positions.

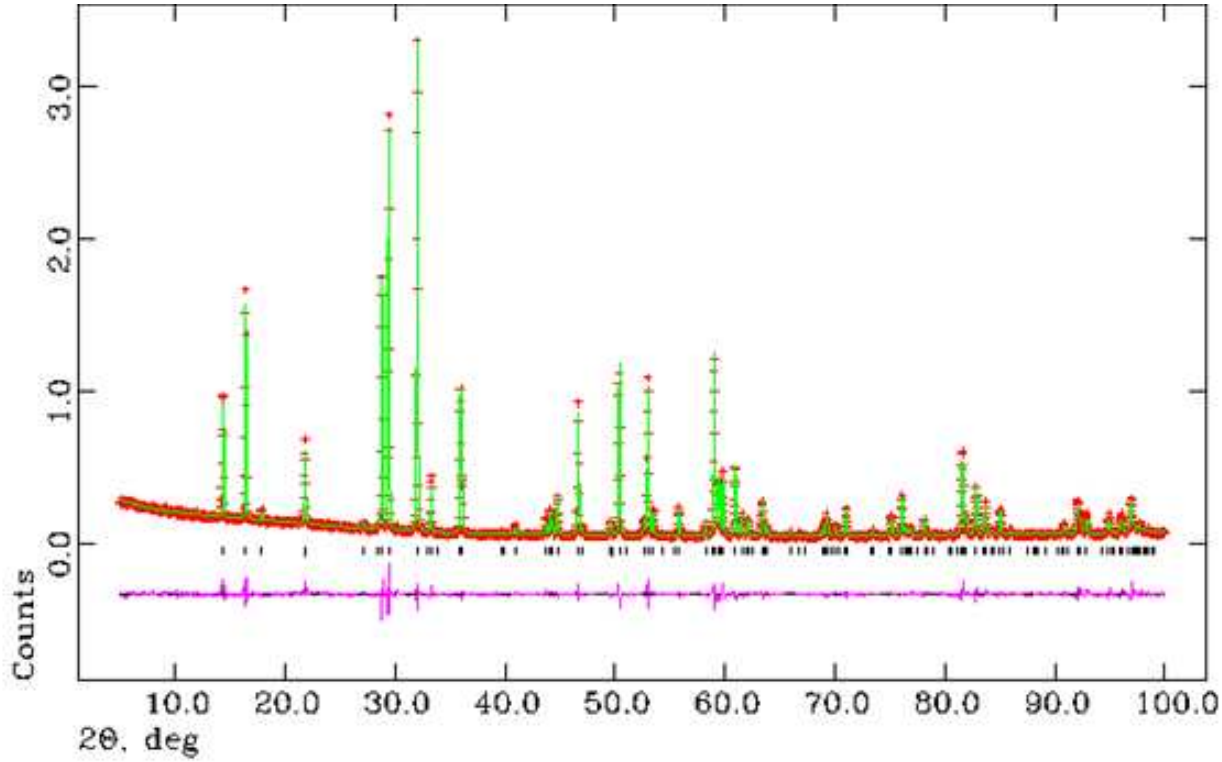

Figure 5: The observed (+), calculated (-) and difference (-) profiles from Rietveld refinement of $PrHfTa_3O_{11}$ with disordered arrangement of Ta, Hf in the ratio 3:1. Ticks marks represent Bragg peak positions.

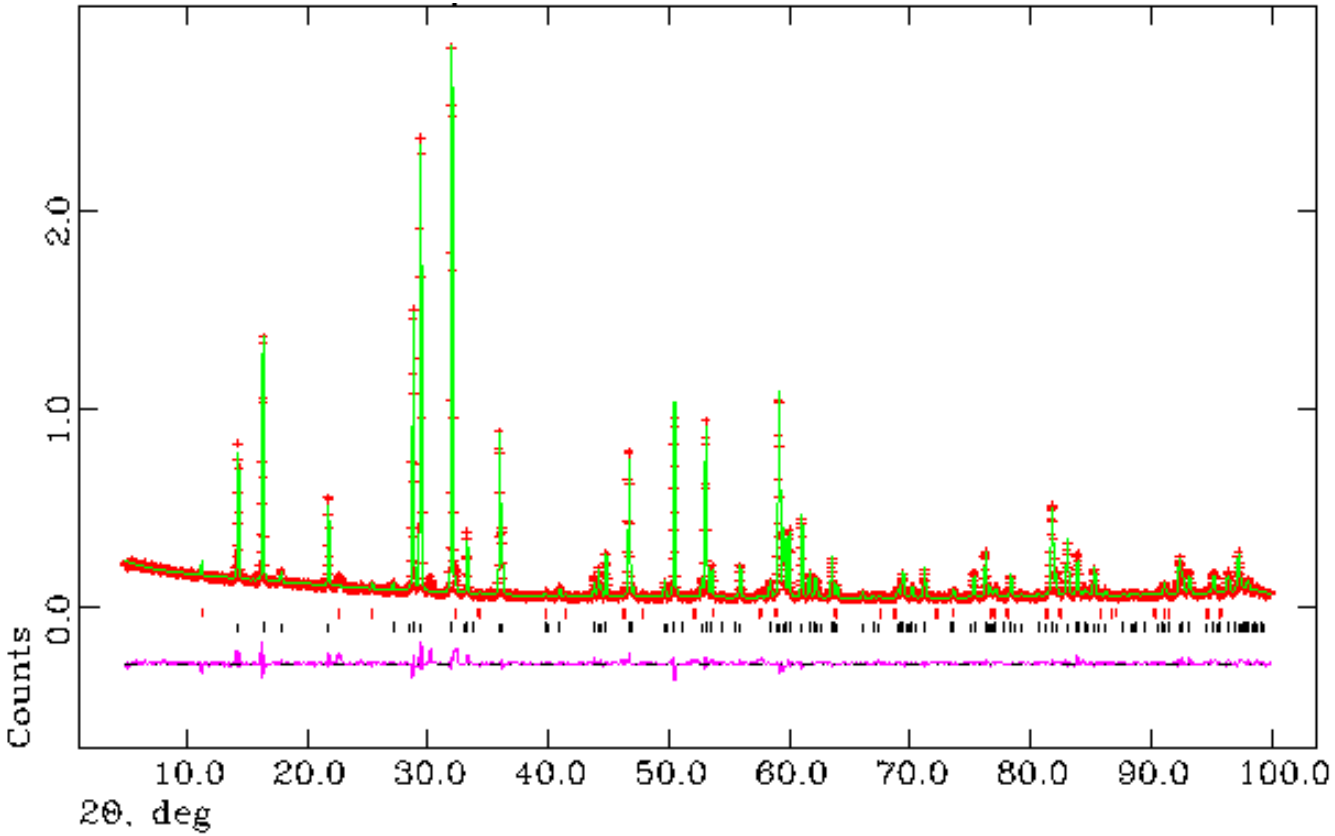

Figure 6: The observed (+), calculated (-) and difference (-) profiles from Rietveld refinement of $NdHfTa_3O_{11}$ with disordered arrangement of Ta, Hf in the ratio 3:1. Ticks marks represent Bragg peak positions.

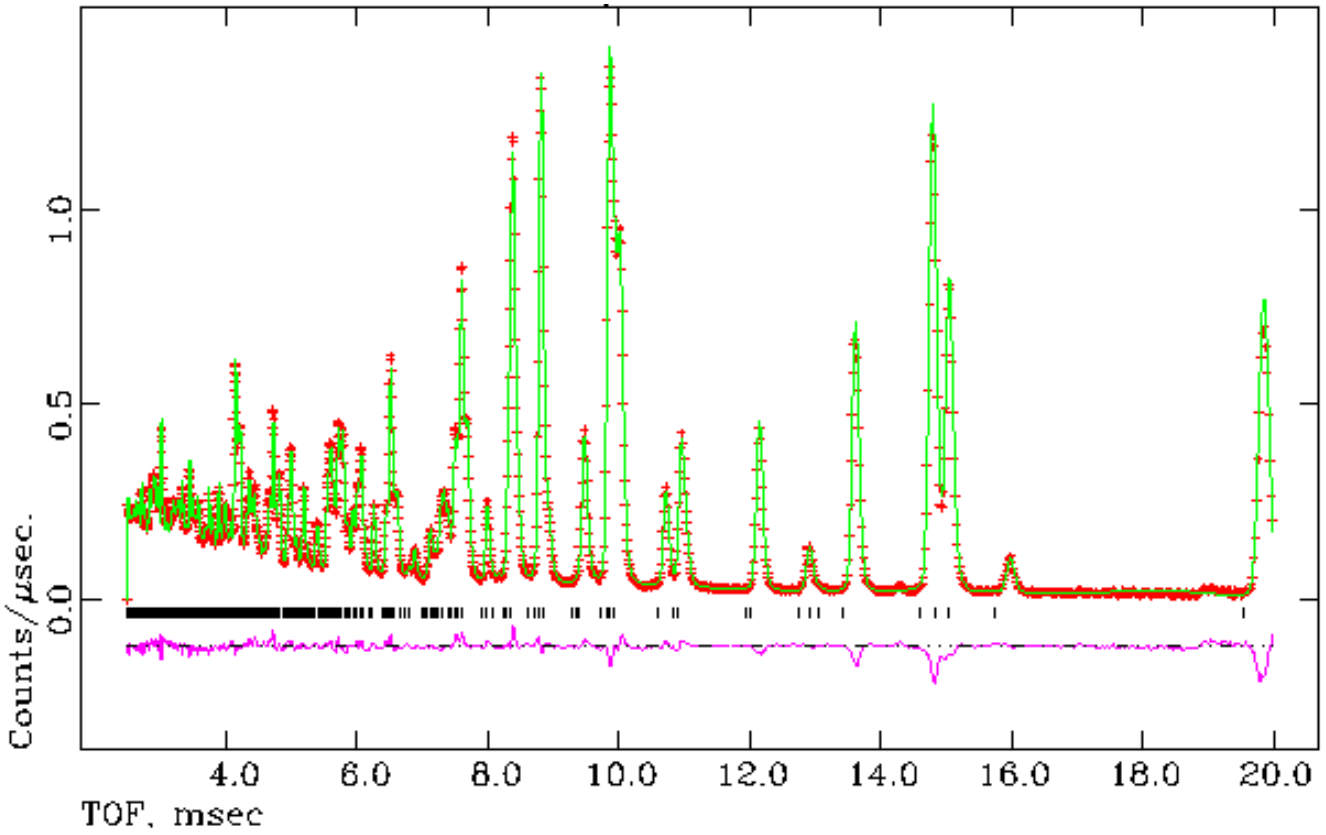

Figure 7: Observed (+), calculated (-) and difference (-) ND profiles at room temperature using constant wavelength ND data of $LaHfNb_3O_{11}$. Tick marks represent Bragg peak positions.

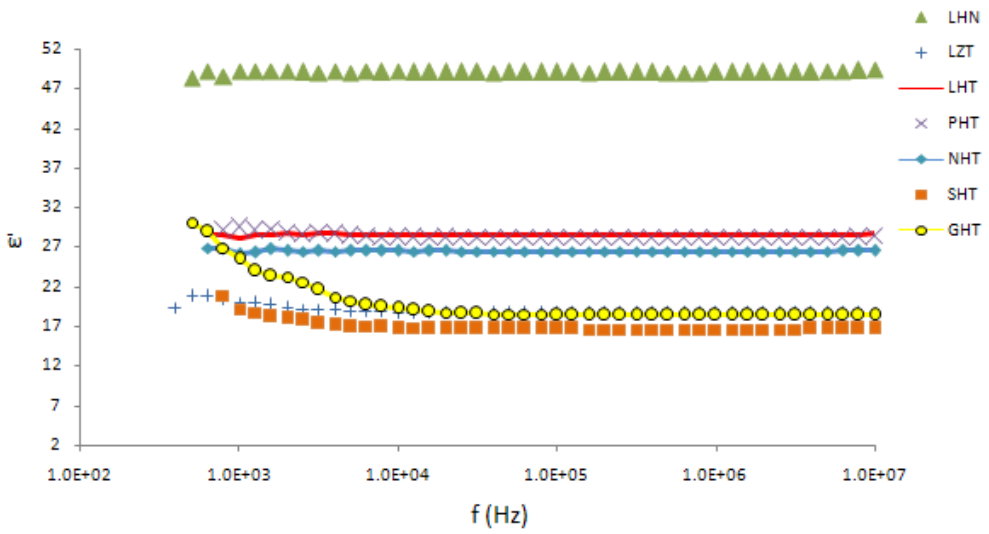

Figure 8: Permittivity, ε', at room temperature for ABC_3O_{11} phases.

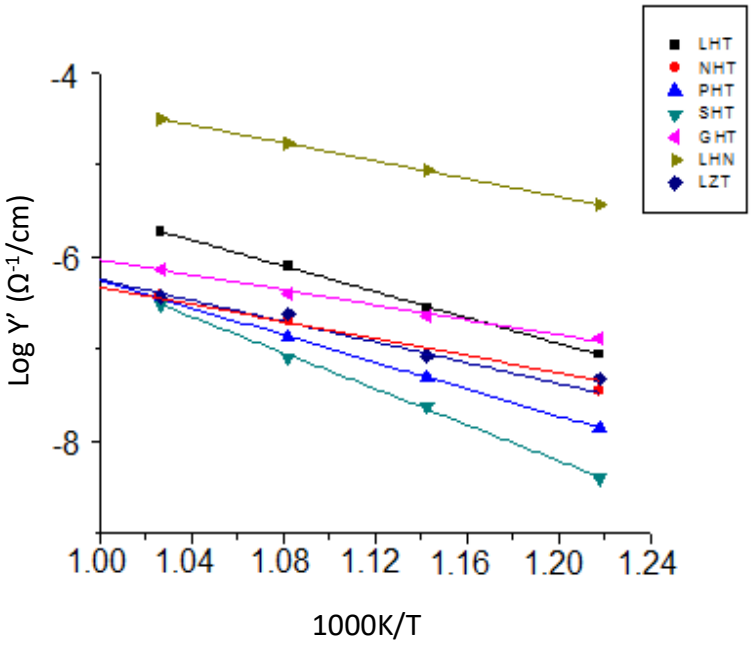

Figure 9: Conductivity data for the new phases.

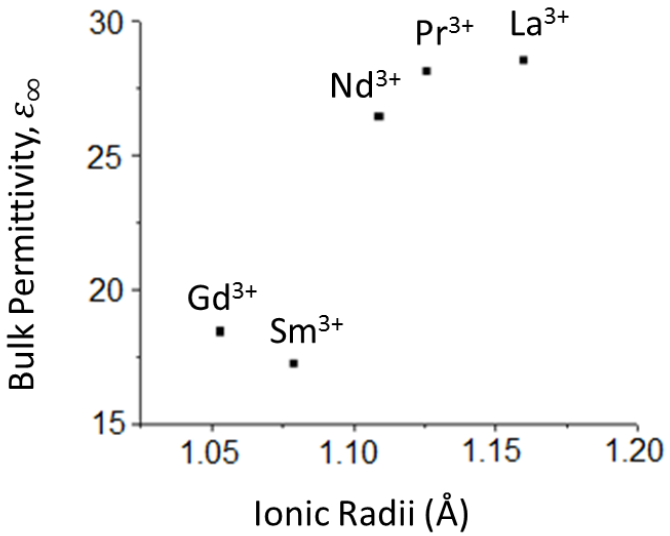

Figure 10: Bulk permittivity of the tantalates phases at room temperature vs. ionic radii of rare earth elements

No.	Compositions	T (^{O}C)	Time (h)	Phases Present
1.	$LaZrTa_3O_{11}$ (LZT)	1500	12	LZT, $LaTa_3O_9$, ZrO_2
		1500	24	LZT, $LaTa_3O_9$, ZrO_2
		1500	36	LZT, $LaTa_3O_9$, ZrO_2
		1500	48	LZT, $LaTa_3O_9$, ZrO_2
		1500	72	LZT, trace of $LaTa_3O_9$ and ZrO_2
2.	$LaHfTa_3O_{11}$ (LHT)	1500	24	LHT, HfO_2
		1500	48	LHT, trace of HfO_2
3.	$LaHfNb_3O_{11}$ (LHN)	1150	24	LHN, Nb_2O_5, La_2O_3, HfO_2
		1250	36	LHN, Nb_2O_5, La_2O_3, HfO_2
		1300	96	LHN, trace of HfO_2
		1350	108	Melt
4.	$LaZrNb_3O_{11}$ (LZN)	1000	12	$La_2Zr_2O_7$, LZN, Nb_2O_5, La_2O_3, ZrO_2
		1150	36	LZN, $LaNb_3O_9$, La_2O_3, ZrO_2
		1150	48	$LaNb_3O_9$, LZN, La_2O_3, ZrO_2
		1200	60	$LaNb_3O_9$, $Nb_2Zr_6O_{17}$
5.	$PrHfTa_3O_{11}$ (PHT)	1350	54	PHT, Ta_2O_5, HfO_2
		1500	78	PHT, Ta_2O_5, HfO_2
		1500	102	PHT, Ta_2O_5, HfO_2
		1500	126	PHT, HfO_2
		1500	150	PHT, trace of HfO_2
6.	$NdHfTa_3O_{11}$ (NHT)	1000	12	Ta_2O_5, $NdTa_7O_{19}$, HfO_2
		1500	24	NHT, Ta_2O_5, HfO_2
		1500	48	NHT, Ta_2O_5, HfO_2
		1500	60	NHT, trace of Ta_2O_5 and HfO_2
7.	$NdHfNb_3O_{11}$ (NHN)	1000	24	$NdNbO_4$, Nb_2O_5, HfO_2, Nd_2O_3
		1100	36	$NdNbO_4$, Nb_2O_5, HfO_2, Nd_2O_3
		1150	72	NHN, $NdNb_3O_9$, HfO_2, Nd_2O_3
		1200	96	$NdNb_3O_9$, NHN, HfO_2, Nd_2O_3
		1250	108	$NdNb_3O_9$, HfO_2, Nd_2O_3
8.	$SmHfTa_3O_{11}$ (SHT)	1200	12	SHT, $SmTa_3O_9$, Ta_2O_5, HfO_2, Sm_2O_3
		1300	24	SHT, $SmTa_3O_9$, Ta_2O_5, HfO_2, Sm_2O_3
		1350	72	SHT, $SmTa_3O_9$, Ta_2O_5, HfO_2
		1375	84	SHT, $SmTa_3O_9$, Ta_2O_5, HfO_2
		1400	96	SHT, $SmTa_3O_9$, Ta_2O_5, HfO_2
		1500	108	$SmTa_3O_9$, SHT, HfO_2
9.	$GdHfTa_3O_{11}$ (GHT)	1200	12	GHT, $GdTa_3O_9$, Ta_2O_5, HfO_2, Gd_2O_3
		1300	24	GHT, $GdTa_3O_9$, Ta_2O_5, HfO_2, Gd_2O_3
		1350	72	GHT, $GdTa_3O_9$, Ta_2O_5, HfO_2
		1375	84	GHT, $GdTa_3O_9$, Ta_2O_5, HfO_2
		1400	96	GHT, $GdTa_3O_9$, Ta_2O_5, HfO_2
		1500	108	$GdTa_3O_9$, LZT, HfO_2

(a)

No.	Compositions	T (^{O}C)	Time (h)	Phases Present
1.	$DyHfTa_3O_{11}$	1000	12	Unknown, $DyTaO_4$, Ta_2O_5, Dy_2O_3, HfO_2
		1300	120	Unknown, $DyTaO_4$, Ta_2O_5, Dy_2O_3, HfO_2
2.	$ErHfTa_3O_{11}$	1000	12	Ta_2O_5, Er_2O_3, HfO_2
		1150	36	$ErTaO_4$, Ta_2O_5, Er_2O_3, HfO_2
		1200	60	$ErTaO_4$, Ta_2O_5, Er_2O_3, HfO_2
		1250	72	$ErTa_7O_{19}$, $ErTaO_4$, Ta_2O_5, HfO_2
3.	$PrHfNb_3O_{11}$	1000	15	$PrNbO_4$, Nb_2O_5, HfO_2, Pr_6O_{11}
		1100	40	$PrNb_5O_{14}$,$PrNb_3O_9$, Nb_2O_5, HfO_2
		1150	60	$PrNb_5O_{14}$, $PrNb_3O_9$, HfO_2
		1300	72	$PrNb_5O_{14}$, $PrNb_3O_9$, HfO_2
4.	$PrZrTa_3O_{11}$	1350	54	$Ta_4Zr_{11}O_{32}$, ZrO_2, Ta_2O_5
5.	$PrZrNb_3O_{11}$	1000	15	$PrNbO_4$, Nb_2O_5, HfO_2, Pr_6O_{11}
		1100	41	$PrNb_5O_{14}$,$PrNb_3O_9$, ZrO_2
		1300	53	$PrNb_5O_{14}$,$PrNb_3O_9$, ZrO_2
6.	$NdZrTa_3O_{11}$	1500	72	$NdTa_3O_9$,$Ta_4Zr_{11}O_{32}$, ZrO_2
7.	$NdZrNb_3O_{11}$	1000	24	$NdNbO_4$, Nb_2O_5, ZrO_2, Nd_2O_3
		1050	36	$NdNbO_4$, Nb_2O_5, ZrO_2, Nd_2O_3
		1150	48	$NdNb_5O_{14}$, Nb_2O_5, ZrO_2, Nd_2O_3
8.	$SmZrNb_3O_{11}$	1000	24	Nb_2O_5, ZrO_2, Sm_2O_3
		1050	36	Nb_2O_5, ZrO_2, Sm_2O_3
		1150	48	Nb_2O_5, ZrO_2, Sm_2O_3
9.	$SmHfNb_3O_{11}$	1000	24	Nb_2O_5, HfO_2, Sm_2O_3
		1100	36	$SmNbO_4$, Nb_2O_5,HfO_2
		1200	60	$SmNbO_4$, Nb_2O_5,HfO_2
10.	$GdHfNb_3O_{11}$	1000	24	$GdNbO_4$, Nb_2O_5, HfO_2, Gd_2O_3
		1050	36	$GdNbO_4$, Nb_2O_5, HfO_2, Gd_2O_3
		1150	48	$GdNbO_4$, Nb_2O_5, HfO_2, Gd_2O_3
11.	$GdZrNb_3O_{11}$	1000	24	$GdNbO_4$, Nb_2O_5, ZrO_2, Gd_2O_3
		1050	36	$GdNbO_4$, Nb_2O_5, ZrO_2, Gd_2O_3
		1150	48	$GdNbO_4$, Nb_2O_5, ZrO_2, Gd_2O_3
12.	$YbZrTa_3O_{11}$	1500	72	Ta_2O_5,Yb_2O_3, ZrO_2

(b)

Table 1: Results of heat treatment on different ABC_3O_{11} combinations; (a) those which yielded an $LaZrTa_3O_{11}$ analogue, (b) those for which an $LaZrTa_3O_{11}$ analogue was not obtained.

Table 2: X-ray powder diffraction data for $LaHfTa_3O_{11}$

2ϑ(obs)	*h k l*	*2ϑ(calc)*	*Obs - calc*	*Int.*	*d (obs) Å*	*d (calc) Å*
14.240	0 0 2	14.229	0.0108	31.0	6.2149	6.2196
16.280	1 0 0	16.287	-0.0066	49.0	5.4402	5.4380
17.797	1 0 1	17.787	0.0106	6.6	4.9798	4.9827
21.709	1 0 2	21.691	0.0187	19.8	4.0904	4.0939
27.050	1 0 3	27.020	0.0296	4.0	3.2937	3.2973
28.728	0 0 4	28.683	0.0454	57.0	3.1050	3.1098
29.328	1 1 1	29.315	0.0131	89.6	3.0428	3.0442
31.910	1 1 2	31.904	0.0054	100.0	2.8023	2.8028
33.170	1 0 4	33.159	0.0119	12.2	2.6986	2.6996
35.868	1 1 3	35.847	0.0217	31.8	2.5016	2.5030
39.613	2 0 3	39.605	0.0076	2.1	2.2733	2.2737
40.819	1 1 4	40.808	0.0103	2.9	2.2089	2.2094
43.638	0 0 6	43.622	0.0157	4.8	2.0725	2.0732
44.029	2 1 0	44.021	0.0085	6.2	2.0550	2.0554
44.647	2 1 1	44.649	-0.0018	8.4	2.0280	2.0279
46.549	1 1 5	46.538	0.0113	27.5	1.9494	1.9499
46.879	1 0 6	46.861	0.0185	3.1	1.9365	1.9372
49.459	2 1 3	49.453	0.0055	4.2	1.8413	1.8415
50.299	3 0 0	50.295	0.0034	32.8	1.8126	1.8127
52.549	3 0 2	52.544	0.0051	4.9	1.7401	1.7403
52.880	1 1 6	52.878	0.0015	31.0	1.7300	1.7301
53.389	2 1 4	53.389	-0.0000	6.3	1.7147	1.7147
55.728	2 0 6	55.710	0.0181	6.5	1.6481	1.6436
58.174	2 1 5	58.173	0.0016	4.0	1.5845	1.5846
58.938	3 0 4	58.928	0.0104	35.6	1.5658	1.5651
59.299	2 2 1	59.285	0.0140	11.6	1.5571	1.5575
59.749	1 1 7	59.747	0.0016	13.4	1.5455	1.5455
60.799	2 2 2	60.806	-0.0076	14.1	1.5223	1.5221
61.400	3 1 0	61.425	-0.0245	5.1	1.5038	1.5032
61.964	3 1 1	61.924	0.0399	4.1	1.4954	1.4973
63.289	2 2 3	63.294	-0.0046	7.9	1.4632	1.4631
63.709	2 1 6	63.705	0.0043	3.1	1.4595	1.4596
65.869	3 1 3	65.840	0.0294	2.1	1.4168	1.4174
68.749	3 0 6	68.732	0.0174	2.7	1.3643	1.3646
69.168	3 1 4	69.170	-0.0013	5.0	1.3571	1.3571
69.928	2 1 7	69.922	0.0060	2.8	1.3442	1.3443
70.932	4 0 2	70.898	0.0332	6.0	1.3276	1.3281
73.344	3 1 5	73.347	-0.0023	2.2	1.2898	1.2897
75.020	1 1 9	75.025	-0.0054	4.9	1.2651	1.2650
75.979	2 2 6	75.975	0.0039	8.8	1.2515	1.2515
76.369	4 0 4	76.396	-0.0269	2.6	1.2450	1.2457
76.790	2 1 8	76.806	-0.0153	2.8	1.2403	1.2400
78.050	3 2 2	78.062	-0.0120	4.4	1.2234	1.2232
78.889	1 0 10	78.876	0.0132	1.8	1.2124	1.2126

Crystal symmetry: hexagonal
Refined cell: $a = 6.28319(6)$ Å, $\alpha = 90.0^o$, ($a = b$)
$c = 12.4358(2)$ Å, $\gamma = 120.0^o$,
$V = 425.173(8)$ Å^3

No.	Phases	Observed unit cell parameters (Å)		Volume (Å^3)
		a	***c***	
1.	$LaZrTa_3O_{11}$ (LZT)	6.28724(4)	12.4525(1)	426.296(5)
2.	$LaHfNb_3O_{11}$ (LHN)	6.2986(2)	12.4189(5)	426.68(3)
3.	$LaHfTa_3O_{11}$ (LHT)	6.28319(6)	12.4358(2)	425.173(8)
4.	$PrHfTa_3O_{11}$ (PHT)	6.281145(8)	12.4412(2)	425.08(3)
5.	$NdHfTa_3O_{11}$ (NHT)	6.2578(1)	12.3938(3)	420.32(2)
6.	$SmHfTa_3O_{11}$ (SHT)	6.23885(8)	12.3569(2)	416.53(1)
7.	$GdHfTa_3O_{11}$ (GHT)	6.2293(1)	12.3421(3)	414.77(2)

Table 3: Lattice parameters and unit cell volumes for ABC_3O_{11} phases

Sites	Properties	$LaHfTa_3O_{11}$	$PrHfTa_3O_{11}$	$NdHfTa_3O_{11}$	$LaHfNb_3O_{11}$
2c (RE Elements)	*(x, y, z)*	0.3333, 0.6667, 0.25	0.3333, 0.6667, 0.25	0.3333, 0.6667, 0.25	0.3333, 0.6667, 0.25
	Uiso	0.3(2)	0.7(2)	0.3(3)	0.50(4)
	Occupancy	1.0	1.0	1.0	1.0
6g (Ta, Hf / Nb)1	*(x, y, z)*	0.6418(2), 0.0, 0.0	0.6414(2), 0.0, 0.0	0.6413(2), 0.0, 0.0	0.6430(1), 0.0, 0.0
	Uiso	0.50(3)	0.61(5)	0.50(5)	0.15(2)
	Occupancy	0.75 / 0.25	0.75 / 0.25	0.75 / 0.25	0.75 / 0.25
2d (Ta, Hf / Nb)2	*(x, y, z)*	0.3333, 0.6667, 0.75	0.3333, 0.6667, 0.75	0.3333 ,0.6667, 0.75	0.3333, 0.6667, 0.75
	Uiso	0.5(1)	0.2(2)	0.3(2)	0.1(4)
	Occupancy	0.75 / 0.25	0.75 / 0.25	0.75 / 0.25	0.75 / 0.25
4f (O1)	*(x, y, z)*	0.3333, 0.6667, 0.39(1)	0.3333, 0.6667, 0.0042(2)	0.3333, 0.6667, 0.043(2)	0.3333, 0.6667,0.388(1)
	Uiso	0.5(2)	0.8(3)	1.7(3)	0.38(3)
	Occupancy	1.0	1.0	1.0	1.0
6g (O2)	*(x, y, z)*	0.244(2), 0.0, 0.0	0.241(2), 0.0, 0.0	0.244(2), 0.0, 0.0	0.2484(2), 0.0, 0.0
	Uiso	0.5(2)	0.8(3)	1.7(3)	0.88(3)
	Occupancy	1.0	1.0	1.0	1.0
12i (O3)	*(x, y, z)*	0.949(2), 0.377(2), 0.3415(6)	0.953(3), 0.382(3), 0.3430(8)	0.953(3), 0.385(3), 0.3420(8)	0.944(1), 0.373(2), 0.34257(6)
	Uiso	0.5(2)	0.8(3)	1.7(3)	0.46(2)
	Occupancy	1.0	1.0	1.0	1.0
a (Å)		6.28320(6)	6.281145(8)	6.2578(1)	6.2986(2)
c (Å)		12.4358(2)	12.4412(2)	12.3939(3)	12.4189(5)
Cell Volume, V ($Å^3$)		425.175(8)	425.08(1)	420.32(1)	426.68(3)
R_{wp} *(%)*		7.02	7.60	6.42	5.73
R_p *(%)*		5.30	5.74	4.389	4.46
χ^2		4.704	7.475	5.996	5.878

Table 4: Structural refinement data for $LaHfTa_3O_{11}$, $PrHfTa_3O_{11}$, $NdHfTa_3O_{11}$ and $LaHfNb_3O_{11}$

Bonding		**No.**	**$LaHfTa_3O_{11}$**	**$PrHfTa_3O_{11}$**	**$NdHfTa_3O_{11}$**	**$LaHfNb_3O_{11}$**
(Ta, Hf / Nb) 1	O1	2×	2.080(4) Å	2.087(5) Å	2.082(5) Å	2.0858(5) Å
	O2	2×	1.992(2) Å	1.988(3) Å	1.986(3) Å	1.9963(7) Å
	O3	2×	2.009(7) Å	1.992(9) Å	1.998(9) Å	1.9979(8) Å
	O2	1×	2.494(9) Å	2.51(1) Å	2.48(1) Å	2.485(2) Å
(Ta, Hf / Nb) 2	O3	6×	2.012(9) Å	2.02(1) Å	2.01(1) Å	2.0014(7) Å
RE Elements	O1	6×	2.61(2) Å	2.44(2) Å	2.56(2) Å	2.622(1) Å
	O3	2×	2.45(1) Å	2.58(2) Å	2.42(1) Å	2.4921(8) Å

Table 5: Selected bond distances of $LaHfTa_3O_{11}$, $PrHfTa_3O_{11}$, $NdHfTa_3O_{11}$ and $LaHfNb_3O_{11}$